The Cleavage Product of Amyloid-β Protein Precursor sAβPPα Modulates BAG3-Dependent Aggresome Formation and Enhances Cellular Proteasomal Activity

Jana Renziehausen[a], Christof Hiebel[a], Heike Nagel[a], Arpita Kundu[b], Stefan Kins[c], Donat Kögel[b], Christian Behl[a,*,1] and Parvana Hajieva[a,*,1]

[a]*Institute for Pathobiochemistry, University Medical Center of the Johannes Gutenberg University Mainz, Mainz, Germany*
[b]*Experimental Neurosurgery, Neuroscience Center, Goethe University Hospital, Frankfurt, Germany*
[c]*Department of Human Biology and Human Genetics, Technical University of Kaiserslautern, Kaiserslautern, Germany*

Handling Associate Editor: Jürgen Götz

Abstract. Alzheimer's disease (AD) is the major age-associated form of dementia characterized by gradual cognitive decline. Aberrant cleavage of the amyloid-β protein precursor (AβPP) is thought to play an important role in the pathology of this disease. Two principal AβPP processing pathways exist: amyloidogenic cleavage of AβPP resulting in production of the soluble N-terminal fragment sAβPPβ, amyloid-β (Aβ), which accumulates in AD brain, and the AβPP intracellular domain (AICD) sAβPPα, p3 and AICD are generated in the non-amyloidogenic pathway. Prevalence of amyloidogenic versus non-amyloidogenic processing leads to depletion of sAβPPα and an increase in Aβ. Although sAβPPα is a well-accepted neurotrophic protein, molecular effects of this fragment remains unknown. Different studies reported impaired protein degradation pathways in AD brain, pointing to a role of disturbed proteasomal activity in the pathogenesis of this disease. Here we studied the possible role of sAβPPα in Bag3-mediated selective macroautophagy and proteasomal degradation. Employing human IMR90 cells, HEK 293 cells, and primary neurons, we demonstrate that sAβPPα prevents the proteotoxic stress-induced increase of Bag3 at the protein and at the mRNA level indicating a transcriptional regulation. Intriguingly, p62 and LC3, two other key players of autophagy, were not affected. Moreover, the formation and the accumulation of disease-related protein aggregates were significantly reduced by sAβPPα. Interestingly, there was a significant increase of proteasomal activity by sAβPPα as demonstrated by using various proteasome substrates. Our findings demonstrate that sAβPPα modulates Bag3 expression, aggresome formation, and proteasomal activity, thereby providing first evidence for a function of sAβPPα in the regulation of proteostasis.

Keywords: Alzheimer's disease, autophagy, Bag3 protein, fibroblasts, proteasome, sAβPPα

---

[1]These authors contributed equally to this work.

*Correspondence to: Christian Behl, PhD, Institute for Pathobiochemistry, University Medical Center of the Johannes Gutenberg University Mainz, Duesbergweg 6, 55099 Mainz, Germany. Tel.: +49 6131 39 25890; Fax: +49 6131 39 25792; E-mail: cbehl@uni-mainz.de and

Parvana Hajieva, PhD, Institute for Pathobiochemistry, University Medical Center of the Johannes Gutenberg University Mainz, Duesbergweg 6, 55099 Mainz, Germany. Tel.: +49 6131 39 24552; Fax: +49 6131 39 25743; E-mail: hajieva@uni-mainz.de.

INTRODUCTION

Alzheimer's disease (AD) is the most common neurodegenerative disorder, which is clinically characterized by a gradual decline of cognitive function and development of dementia. Although familiar forms of AD have mostly an early age of onset, the sporadic forms of this disease are strictly age-associated. AD is characterized by two distinct neuropathological hallmarks, an accumulation of extracellular amyloid plaques and intracellular neurofibrillary tangles [1, 2]. The amyloid-β protein precursor, AβPP, whose processing at the β, γ, and caspase cleavage sites results in the generation of four pro-AD-peptides: soluble AβPP beta (sAβPPβ), βCTF, which in turn can be cleaved to amyloid-β (Aβ), and the intracellular domain AICD as well as Jcasp [3]. In contrast, cleavage at the α site produces the trophic peptide soluble AβPP alpha (sAβPPα) and the inhibitor of AβPP γ-site cleavage, alpha-C-terminal fragment of AβPP (αCTF) [4, 5]. The molecular switch between neurotrophic α cleavage and the neurotoxic combined β-/, γ- as well as caspase cleavage is considered to play an important role in the etiology and pathogenesis of AD. Soluble sAβPPα is proposed to have neurotrophic and neuroprotective properties, possibly counteracting the neurotoxic effects of Aβ [6, 7]. Accordingly, loss of sAβPPα was observed in patients with AD pathology as compared to aged-matched controls [8–10]. Strategies directed at increasing the activity of non-amyloidogenic processing of AβPP through α-secretase, have been suggested to be a promising therapeutic approach [11]. Two regions on the peptide sequence of sAβPPα are identified as being required for its neuroprotective activity, the N-terminal E1 and E2 domain respectively, both of which contain heparin binding activity [12]. The ability of sAβPPα to bind heparin sulphate proteoglycans through its heparin binding site within the E1 domain is thought to define its neuroprotective properties [12]. The neuroprotective and neurotrophic effect of sAβPPα was demonstrated in various *in vivo* and *in vitro* experimental models [13, 7]. However, the exact intracellular molecular targets of sAβPPα -mediated cytoprotection are not yet fully defined. Recent studies demonstrated that sAβPPα -dependent neuroprotection involves activation of the pro-survival PI3K/Akt pathway and inhibition of stress-triggered JNK activation [14, 15]. Intriguingly, inhibition of JNK/cJun signaling decreases the expression of the co-chaperone protein Bag3 [16]. Bag3 is a member of the Bcl-2-associated athanogene family that can be stimulated during cellular responses to stressful conditions, such as oxidative stress and proteasome inhibition [17]. Our previous investigations demonstrated an expression switch from Bag1 to Bag3 during cell aging. While Bag1 is involved in proteasomal degradation in young cells Bag3 induces a selective macroautophagy pathway during cellular aging and oxidative stress [17]. Lysosomal activity is essential for complete degradation of cargo in the autophagic pathway. Given the fact that the pathology of AD is accompanied by a lysosomal dysfunction (for review, see [18]), we have investigated the potential effect of sAβPPα on the crosstalk between proteasomal and autophagic protein degradation machineries. Employing primary fibroblasts IMR90, HEK 293 as well as rat primary hippocampal neurons, we investigated the efficacy of sAβPPα on the intracellular adaptation to proteotoxic stress. Our results demonstrate that sAβPPα prevents the upregulation of Bag3 protein and Bag3-mediated aggresome formation induced under conditions of proteasomal stress. This sAβPPα -induced reduction of Bag3 levels was accompanied by a significant increase of the proteasomal activity. Interestingly, this activity could be observed in young IMR90 cells and primary neuronal cultures, but not in aged IMR90 revealing differential effects of sAβPPα in young and aged cells.

Our data support the view that the increased generation of sAβPPα as a product of α-secretase cleavage may enhance the turnover of damaged/accumulated proteins via modulation of proteasomal activity. These findings provide a completely novel function of sAβPPα in enhancing the cellular capacity to adapt to proteotoxic stress, thereby contributing to the cytoprotective activity of AβPP.

MATERIALS AND METHODS

Materials

MG-132 was purchased from Calbiochem and Bafilomycin A1 from LC Laboratories. Both compounds were dissolved in DMSO. Proteasome substrate SUC-LLVY-AMC was from Enzo. Cell culture media and supplements were from Invitrogen unless otherwise stated. FuGENE Transfection Reagent was from Promega.

Cell culture

Primary human fibroblasts IMR90 were purchased from Coriell Institute for Medical Research and human embryonic kidney cells (HEK 293) were from the

American Type Culture Collection (ATCC). HEK 293 cells stably expressing a GFP-based UPS reporter (d2-GFP) was established in our laboratory and used as described previously [17].

IMR90 cells were cultivated in Dulbecco's modified Eagle's medium (DMEM) with low glucose (1 g/L) and 1 mM sodium pyruvate and supplemented with 10% heat-inactivated fetal calf serum (FCS), antibiotics, and antimycotics. At subconfluency, cells were passaged by trypsinization. Population doubling levels (PDL) were calculated as (logCh -logCs)/log (2), where Ch and Cs are defined as the cell number harvested and seeded, respectively. The aged phenotype was identified by use of a senescence-associated galactosidase staining kit (Cell Signaling), following the manufacturer's instructions.

HEK 293 cells were cultivated in DMEM with high glucose (4.5 g/L) supplemented with 10% heat-inactivated FCS, 1 mM sodium pyruvate, antibiotics, and antimycotics.

Cell survival assay

Young and aged IMR90 cells were seeded into 96-well plates with 10^4 cells per well in 0.1 ml medium. Following 24 h of cultivation cells were pre-treated with different concentrations of sAβPPα for 24 h. Afterwards, they were challenged with 0.5 μM MG-132 and cultivated for 72 h. Cell viability was quantified by measuring the metabolic activity by cellular tetrazole reduction as published previously [19]. For that, MTT solution (0.5 mg/ml) was added to the cultures for 4 h, after which the cells were lysed with 0.1 ml solubilization solution (40% dimethylformamide, 20% sodium dodecyl sulfate (SDS), pH 4.0 adjusted with acetic acid). Approximately 6 h later, the absorbance of the reduced MTT formazan crystals was measured photometrically at 560 nm (Multiskan from Thermo Fisher Scientific, Waltham, MA, USA).

Transient transfections

HEK 293 cells were transfected with SOD1^{G85R}-GFP plasmid using FuGENE Transfection reagent according to the manufacturer's instructions. HEK 293 cells were seeded on glass cover slips for 24 h and then transfected with 1 μg plasmid.

For knock down experiments, IMR90 cells were transiently transfected with small interfering RNA (siRNA). For that, cell suspension was transfected with 60 μg siRNAs by electroporation and then was seeded in 96 well plates. The experiment was performed 24 h post transfection. The following siRNA sequences were used: GCAAAGAGGUGGAUU-CUAA (dTdT) and UUAGAAUCCACCUCUUUGC (dTdT) for Bag3 (purchased from Sigma) and AUU-CUCCGAACGUGUCACG (dTdT) (purchased from MWG Eurofins) as a control "non-sense" RNA.

Immunoblotting

Cells were harvested with lysis buffer (50 mM Tris-HCl, pH 6.8; 2% sodium dodecyl sulfate and 10% sucrose plus protease- and phosphatase inhibitor) and briefly sonicated. Protein concentration was determined using BCA kit (Pierce) according to manufacturer's protocol. 20 μg of total cell lysate were loaded on 12% SDS-PAGE and separated with Mini protean III system (Bio-Rad). Afterwards, proteins were transferred onto nitrocellulose membrane by electroblotting. Following 30 min incubation with 5% low fat milk to block non-specific binding sites, membranes were incubated with the following primary antibodies: rabbit anti-Bag3 (1 : 500, Proteintech group); mouse anti-Lamp2 (1 : 500, Abcam); rabbit anti-LC3b (1 : 500, Sigma-Aldrich); mouse anti-Nrf2 (1 : 500, Abcam); guinea pig anti-p62 (1 : 500; Progen); rabbit anti-proteasome 19S (1.500; Abcam) and 20S (1 : 500, Santa Cruz Technology); rabbit anti-ubiquitin (1 : 500; Dako). The cBAG antibody was raised in rabbits against human BAG domain in BAG1M (aa 151–263) and was used as previously published [17]. This antibody was kindly provided by Prof. Ulrich Hartl (Department of Cellular Biochemistry, Max-Planck-Institute of Biochemistry, Martinsried, Germany). Anti-α-tubulin (1 : 1000; Sigma-Aldrich) immunoreactive signal was used as a control for equal protein loading. Primary antibodies were detected with horseradish peroxidase conjugated secondary antibodies. All antibodies and the low fat milk powder used were in Tris-buffered saline/Tween-20 (TBST). The densitometric analysis of the immunoreactive bands was performed using Image J Software. After densitometric quantification, the obtained absolute values were first normalized to tubulin, which was used as a control for equal protein loading.

Immunocytochemistry

HEK 293 cells were grown on glass cover slips coated with 0.1 mg/ml poly-L-ornithine (MW 30–70 kDa, Sigma) and fixed with 4% paraformaldehyde. Unspecific epitopes were blocked with 3% BSA and cells were subsequently permeabilized with 0.1%

Triton X-100. At this point, cells were incubated overnight with primary antibody (rabbit anti-Bag3 diluted 1:100 with PBST) in PBS containing 1% BSA. After that, cells were incubated with AlexaFluor647 conjugated secondary antibody. Cell nuclei were counterstained with 4, 6-diamidino-2-phenylindole (DAPI) (l μg/mL in PBS for 20 min). Cells were analyzed and photographed using a confocal laser-scanning microscope LSM710 (Zeiss).

Quantitative real-time RT-PCR

Total RNA was isolated using Nucleospin RNA II Kit (Machery-Nagel) and complementary DNA (cDNA) was synthesized with Omniscript RT Kit (Qiagen). Both kits were used according to the manufacture's instructions.

qPCR were performed with 1 μl cDNA, 100 pM of forward and reverse primer (MWG Eurofins), 12.5 μl SensiMix SYBR and Fluorescein Kit (Bioline), and 10.5 μl water in the iCycler (Bio-Rad). Primer sequences are listed below in Table 1.

After initial denaturation (95°C, 15 min), the conditions of the PCR were 20 s 95°C, 20 s 60°C, and 30 s 72°C for 35 cycles. The first PCR cycle with a fluorescence signal above the threshold (C_t) was determined. The results were normalized to a housekeeping gene glycerinaldehyde-3-phosphate dehydrogenase (GAPDH).

Measurement of proteasome activity

IMR90 and HEK 293 cells were washed with ice cold PBS, trypsinized and collected by centrifugation at 200 g for 4 min. The resulting cell pellet was re-suspended in hypotonic buffer (10 mM HEPES, 10 mM potassium acetate, 1.45 mM magnesium acetate, and 1 mM DTT) and incubated for 30 min. Afterwards lysates were passed ten times

Table 1
Primer sequences used for RT-PCR

GAPDH forward	5′- GCA CCA CCA ACT GCT TAG CAC -3′
GAPDH reverse	5′- CAC CAC CTT CTT GAT GTC ATC -3′
Bag3 forward	5′- TGG GAG ATC AAG ATC GAC CC -3′
Bag3 reverse	5′- GGG CCA TTG GCA GAG GAT G -3′
p62 forward	5′- TGC CCA GAC TAC GAC TTG TG -3′
p62 reverse	5′- AGT GTC CGT GTT TCA CCT TCC -3′
PSMB5 forward	5′- AGG TTC TGG CTC TGT GTA TGC -3′
PSMB5 reverse	5′- CAT CTC TGT AGG TGG CTT GGT -3′
PSMB6 forward	5′- GAG GCA TTC ACT CCA GAC TG -3′
PSMB6 reverse	5′- CAA ACT GCA CGG CCA TGA TA -3′
PSMB7 forward	5′- TGC AAA GAG GGG ATA CAA GC -3′
PSMB7 reverse	5′- ACA ACC ATC CCT TCA GTT GC -3′

through a 25-gauge needle and centrifuged at 640 g for 5 min. The supernatants were collected and the concentration of potassium acetate was adjusted to 90 mM. The protein concentration was determined using BCA kit (Pierce) according to manufacturer's protocol and 2.5 μg of protein was mixed with assay buffer (15 mM HEPES, 130 mM potassium acetate, 1.5 mM magnesium acetate, 1.5 mM calcium chloride, 2 mM DTT, and 8 mM ATP) and 0.1 mM SUC-LLVY-AMC. The generated fluorescence was measured in a black 96-well-plate at 37°C every hour using the Victor^3 V Multilabel counter (Perkin Elmer) equipped with excitation 360 nm and emission 460 nm fluorescence filter pair.

Expression and purification of sAβPPα and AβPP fragment E1

The yeast *Pichia pastoris GS115 cells* were used as expression system for sAβPPα and the AβPP fragment E1 (aa 18–189). *P. pastoris* cells were transfected with pBLHIS-SX-based expression vectors encoding for 6xHis-tagged sAβPPα and 6xHis-tagged E1.

For expression of sAβPPα and AβPP E1, the yeast cells were cultivated in BMGY-Media (1% yeast-extract, 2% peptone, 100 mM monopotassium phosphate buffer, 1.34% yeast nitrogen base, 0.0004% biotin, and 1% glycerol) at 30°C with continuous shaking at 300 rpm. After the culture reached the log phase, the yeast cells were harvested by centrifugation at 1500 g for 5 min and resuspended in BMMY media (1% yeast-extract, 2% peptone, 100 mM monopotassium phosphate buffer, 1.34% yeast nitrogen base, 0.0004% biotin and 1% methanol). After incubation for one day at 30°C with 300 rpm shaking the supernatant was collected by centrifugation at 1,500 g for 10 min. sAβPPα and AβPP E1 were purified by fast protein liquid chromatography (FPLC). Bio-scale^{TM} Mini Profinity^{TM} IMAC column (Bio-Rad) was used in the Biologic Duo Flow machine (Bio-Rad). After equilibration of the column with binding buffer A (300 mM potassium chloride, 50 mM potassium phosphate, and 5 mM imidazole), the supernatant was loaded onto the column. After washing with binding buffer A fusion proteins were eluted with elution buffer (300 mM potassium chloride, 50 mM potassium phosphate, 250 mM imidazole). Protein concentration was determined using Pierce 660 nm Protein Assay kit (Thermo Scientific) following the manufacturer's instructions.

Primary neuronal culture

Primary embryonic (E17) neuronal cultures from Sprague Dawley rats were prepared as previously described [19, 20]. In brief, rats were dissected, hippocampi and cortex tissue pieces were collected separately and digested for 20 min in PBS containing 0.1% trypsin and 0.02% EDTA at 20°C, after which the contained cells were gently dissociated and non-dissociated matter, was filtered through Nybolt mesh. After centrifugation at 200 g for 4 min, the cell pellet was resuspended in Neurobasal medium containing 0.1 B27 supplement, 1 mM glutamax, and 5 g/mL gentamicin. For cultivation, the cells were seeded in plates that had been pre-coated with 0.1 mg/mL poly-L-ornithine (MW range 100–200 kDa, from Sigma). Experiments were carried out after 7 days of differentiation *in vitro*.

Statistical analysis

All data are expressed as mean ± standard deviation (SD) of the indicated number of independent experiments performed. Statistically significant differences between the treatment groups were identified by one-way ANOVA followed by Tukey's multiple comparisons test. Significant differences between treatment groups are indicated with single symbols denoting $p \leq 0.05$, double symbols denoting $p \leq 0.01$ and triple symbols denoting $p \leq 0.001$.

RESULTS

sAβPPα prevents the upregulation of Bag3 after proteasomal stress in young but not in aged IMR90 cells

Since the maintenance of intracellular protein homeostasis is essential for cellular viability and function, activation of pro-survival pathways by sAβPPα might be exerted partially through the modulation of protein degradation machinery. To test this hypothesis, we examined the effect of sAβPPα and its N-terminal domain AβPP E1 on Bag3 after proteasomal inhibition. MG-132 was used as a well-established proteasome inhibitor and a known trigger for autophagy. Human primary fibroblasts IMR90 in different stages of replicative senescence were used. These cells represent a well-characterized model of cellular aging [21, 22]. Young (PDL 30) cells were pre-treated with different concentrations of recombinantly expressed and isolated sAβPPα or AβPP E1 for 15 h and challenged with 0.5 μM MG-132. Subsequent analysis of the cells

by means of western blotting revealed a significant induction of Bag3 by MG-132, which was prevented by sAβPPα in a concentration dependent manner starting at 25 nM. However, the strongest influence was detected at 100 nM concentration of sAβPPα (Fig. 1A, B). Accordingly, sAβPPα showed a dose-dependent protective effect against proteotoxic stress as detected by increased cell survival (Fig. 1C). AβPP E1 was used as control peptide that was likewise recombinantly expressed and purified. AβPP E1 had no significant effect on cell survival (Fig. 1D). Importantly, a sole addition of sAβPPα and AβPP E1 had no significant consequence on Bag3 protein levels as well as on cell survival (Fig. 1). In order to investigate a direct involvement of Bag3 on the observed effect of sAβPPα we performed siRNA-mediated knock down experiments for Bag3 protein expression. Interestingly, sAβPPα-mediated effect on cell survival under conditions of proteotoxic stress was observed also in the absence of Bag3 indicating that this effect is independent of Bag3 expression (Fig. 1E).

Interestingly, analysis of young and aged IMR90 cells revealed that the observed effect of both peptides on Bag3 after proteasome inhibition in young IMR90 cells was not confirmed in aged IMR90 cells indicating that young and aged cells use different stress response (Fig. 2A-D). Importantly, the steady-state level of Bag3 protein was significantly higher in aged cells as compared to young cells (Fig. 2G, H). This result is in compliance with our previous work reporting a Bag1/Bag3 expression switch in aged IMR90 cells [17]. In order to investigate whether the influence of sAβPPα on Bag3 expression levels might be exerted on the transcriptional level, we performed quantitative real-time PCR in young and aged IMR90 cells treated under the same conditions as described above. Indeed, application of sAβPPα together with a proteotoxic stress significantly reduced the mRNA levels of Bag3 indicating to a transcriptional regulation of Bag3 expression by sAβPPα (Fig. 2E). Consistent with western blotting analysis, there was no significant effect of sAβPPα in aged IMR90 cells (Fig. 2F).

sAβPPα prevents Bag3 upregulation in primary cortical and hippocampal neurons

In order to investigate the influence of sAβPPα on differentiated neuronal cells, we have employed primary neurons isolated from hippocampus or cortex. The hippocampal and cortical cultures were pre-treated with or without 100 nM sAβPPα. 24 h later the cells were exposed to proteotoxic stress with 10 μM
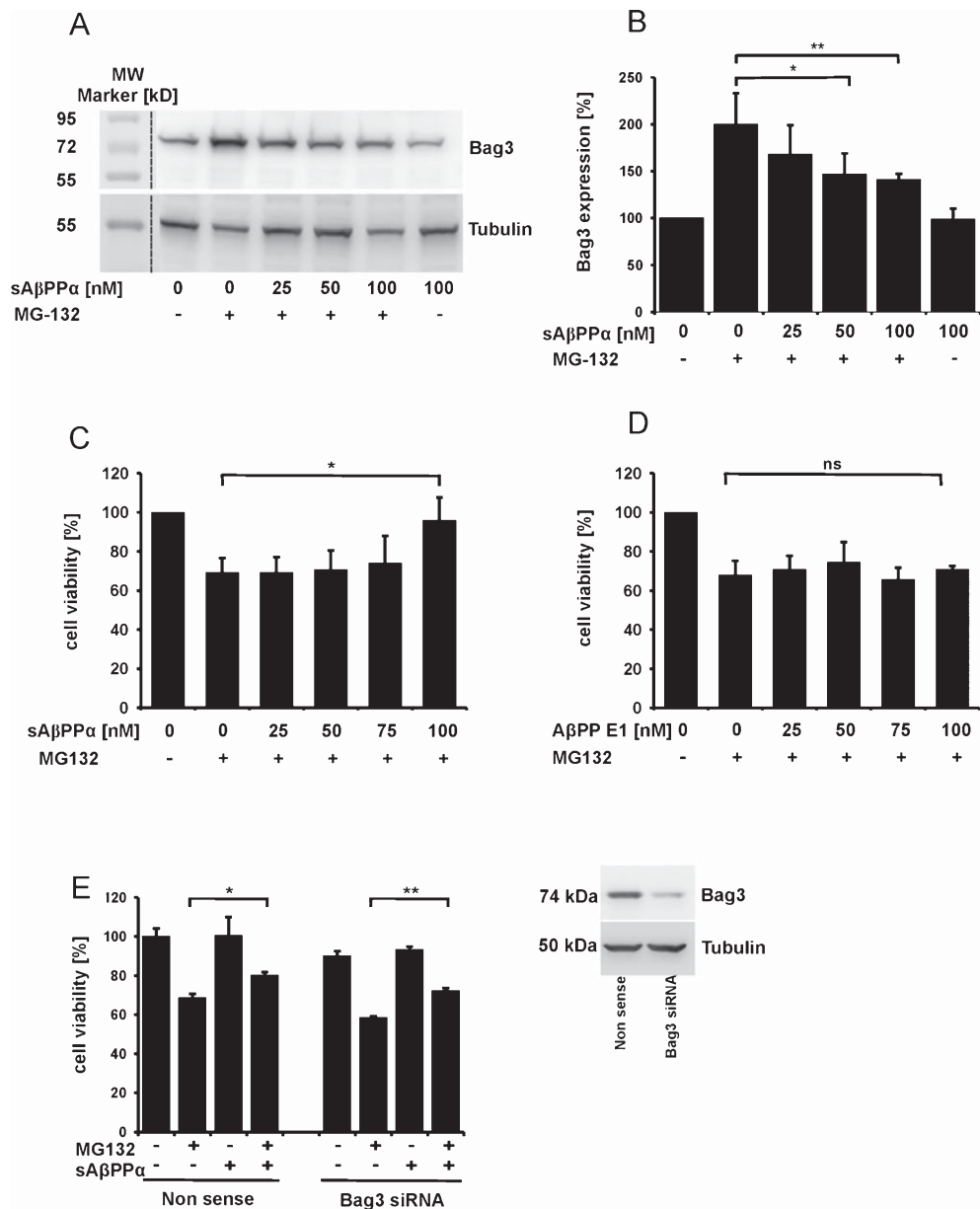
Fig. 1. Dose dependent effects of sAβPPα under MG-132-induced proteotoxic stress. A) IMR90 cells were pre-treated with different concentrations of sAβPPα for 15 h. After that cells were challenged with MG-132 for 24 h. At this point, cells were harvested and total cell lysate was analyzed using western blotting and immunodetected with anti-Bag3 antibody. Tubulin was used as a loading control. B) Densitometric quantification of the immunoreactive bands from (A). The absolute values measured were first normalized to tubulin and the resulting values were normalized to vehicle-treated control, which was set as 100%. Data represent mean ± SD from quadruplicate experiments. Statistically significant differences versus MG-132 only-treated cells are indicated by asterisks: $^*p \leq 0.05$ and $^{**}p \leq 0.01$. C, D) Young IMR90 cells were pre-treated with different concentrations of sAβPPα or AβPP E1 for 24 h. After that cells were challenged with a proteasome inhibitor MG-132 for 48 h. Subsequently cells viability was determined using calorimetric MTT assay. The absolute values measured were normalized to untreated control, which was set as 100%. Data represent mean ± SD from triplicate experiments. Statistically significant differences versus MG-132 only-treated cells are indicated by an asterisk: $^*p \leq 0.05$. E) IMR90 cells were transfected with indicated siRNAs for 24 h. After that cells were pre-treated with 100 nM concentration of sAβPPα and 24 h later the cell viability was determined using MTT cell survival assay. The efficiency of siRNA-mediated knock down was checked by detection of Bag3 immunoreactivity. Statistically significant differences versus MG-132 only-treated cells are indicated by $^*p \leq 0.05$ and $^{**}p \leq 0.01$.
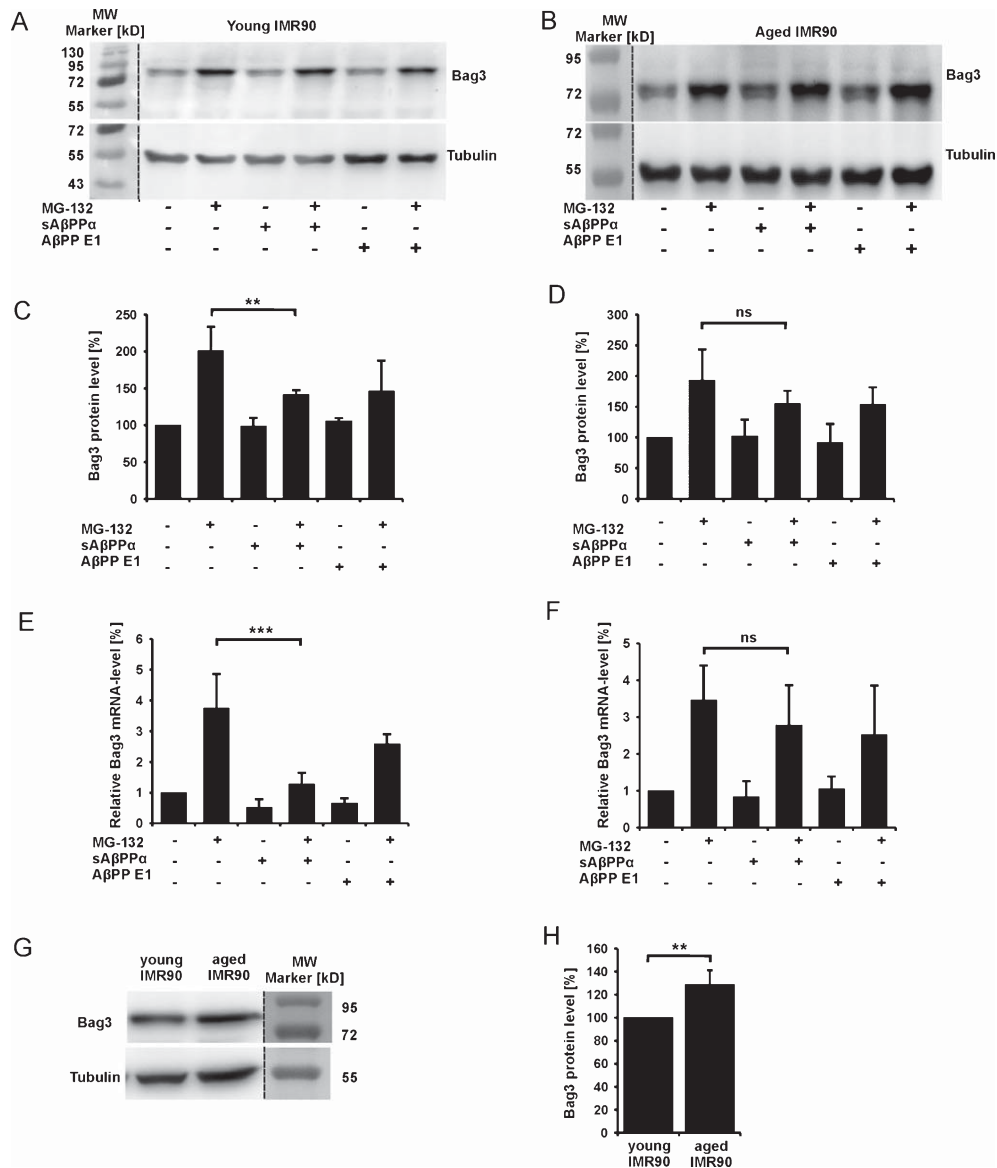
Fig. 2. sAβPPα prevents Bag3 induction under conditions of proteotoxic stress in young IMR90 cells at protein and mRNA levels. A, C, E) Young (PDL <30) and (B, D, F) aged IMR90 (PDL >48) cells were pre-treated with 100 nM sAβPPα and AβPP E1 15 h prior to the administration of 0.5 μM proteasome inhibitor MG-132 for 24 h. Afterwards, the cells were harvested and total cell lysates were subjected for protein extraction and western Blot analysis (A, C) or for mRNA isolation (E, F). Protein extracts were analyzed by western blotting using anti-Bag3 and anti-Tubulin antibodies. C, D) Quantitative densitometric analysis of immunoblots in which Bag3 immunoreactive signal was first normalized to tubulin and the resulting values were normalized to vehicle-treated control, which was set as 100%. Significant differences versus MG-132-only treated controls are marked by double asterisks; $p \leq 0.01$. Data represent mean $\pm$ SD from quadruplicate determinations. E, F) The relative mRNA levels were determined by quantitative PCR analysis. The date represent mean $\pm$ SD from four independent determinations; statistically significant difference is denoted with triple asterisks; $p < 0.001$. G) Determination of the steady-state levels of Bag3 by analyzing the total cell lysates from young (PDL <30) and aged IMR90 (PDL >48) cells by means of western blotting using anti-Bag3 and anti-tubulin antibodies, which was used as a control for equal protein loading. H) Quantitative densitometric analysis of Bag3 protein levels from three independent experiments. For that the Bag3 immunoreactive signal was measured and the values were normalized to tubulin. Bag3 protein level in young IMR90 cells was set as 100%. Significant differences in Bag3 levels between aged and young cells is indicated by double asterisks; $p \leq 0.01$.
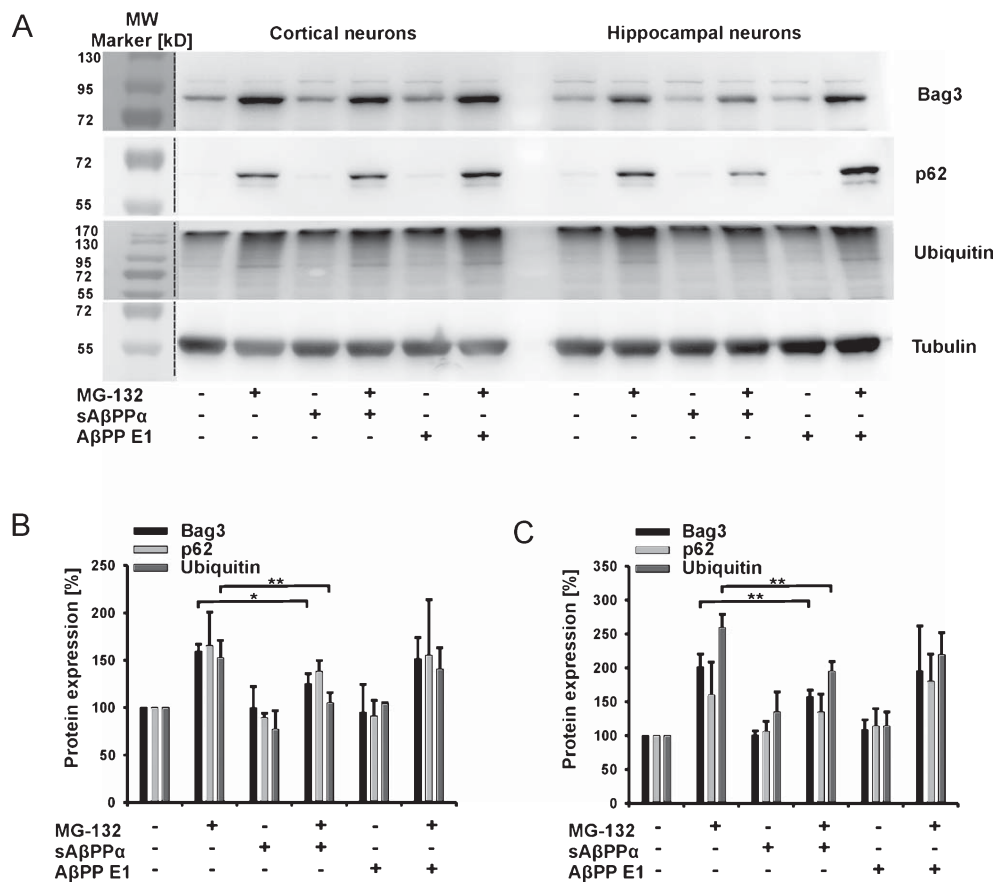
Fig. 3. sAβPPα prevents Bag3 induction under conditions of proteotoxic stress in primary cortical and hippocampal neurons. Primary neuronal cultures from cerebral cortex or hippocampus were pre-treated with sAβPPα or AβPP E1 after 7 days *in vitro* for 15 h. At this point, cells were challenged with or without 10 μM MG-132 and harvested 24 h later. The total cell lysates were immunoblotted using anti-Bag3, anti-p62, anti-ubiquitin antibodies. A) A representative blot showing the immunoreactive bands from cortical neurons (left six lanes and hippocampal neurons (right six lanes); B, C) Densitometric analysis of the immunoreactive bands for cortical and hippocampal neurons. The absolute measured values for Bag3, p62, ubiquitin were first normalized to tubulin and then normalized to vehicle-treated control which was set as 100%. Data represent mean ± SD from triplicate experiments. Statistically significant differences versus MG-132 only-treated cells are indicated by asterisks: *$p \leq 0.05$ and **$p \leq 0.01$.

MG-132 for 48 h. Our results demonstrate a significant induction of MG-132-induced Bag3 expression in primary neurons from both brain regions, which could be prevented by sAβPPα as analyzed by western blotting. Moreover, we measured a significant reduction of protein ubiquitination indicating an increased proteasome activity in sAβPPα -treated neuronal cultures (Fig. 3).

sAβPPα has no influence on the downstream markers of autophagy after proteotoxic stress

The Bag3-mediated selective macroautophagy involves the activation of different downstream target proteins. We examined the effect of sAβPPα and AβPP E1 on the two autophagy-related proteins p62 and Lamp2. The protein p62 is a well described receptor for autophagy substrates triggering the degradation

of polyubiquitinated proteins by simultaneously binding these proteins and LC3 [23]. Analysis of protein levels for p62 in young IMR90 cells revealed that there was no discernible effect of sAβPPα on this protein (Fig. 4A-D). However, the mRNA levels of p62 decreased after proteasomal stress with sAβPPα similar to that of Bag3 (Fig. 4E). In contrast, pre-treatment with AβPP E1 did not lead to significant reductions in the mRNA levels of both genes (Fig. 4F).

Additionally, we investigated whether sAβPPα exerts any effect on LC3-II, which is a prominent autophagosomal marker triggering the fusion of autophagosomes with lysosomes. Given the high turnover rate for LC3-II, we also blocked the autophagic flux by treating the cells with 0.5 μM Bafilomycin A (BafA) for 4 h. Western blot analysis of LC3-II protein levels indicated a slight decrease in
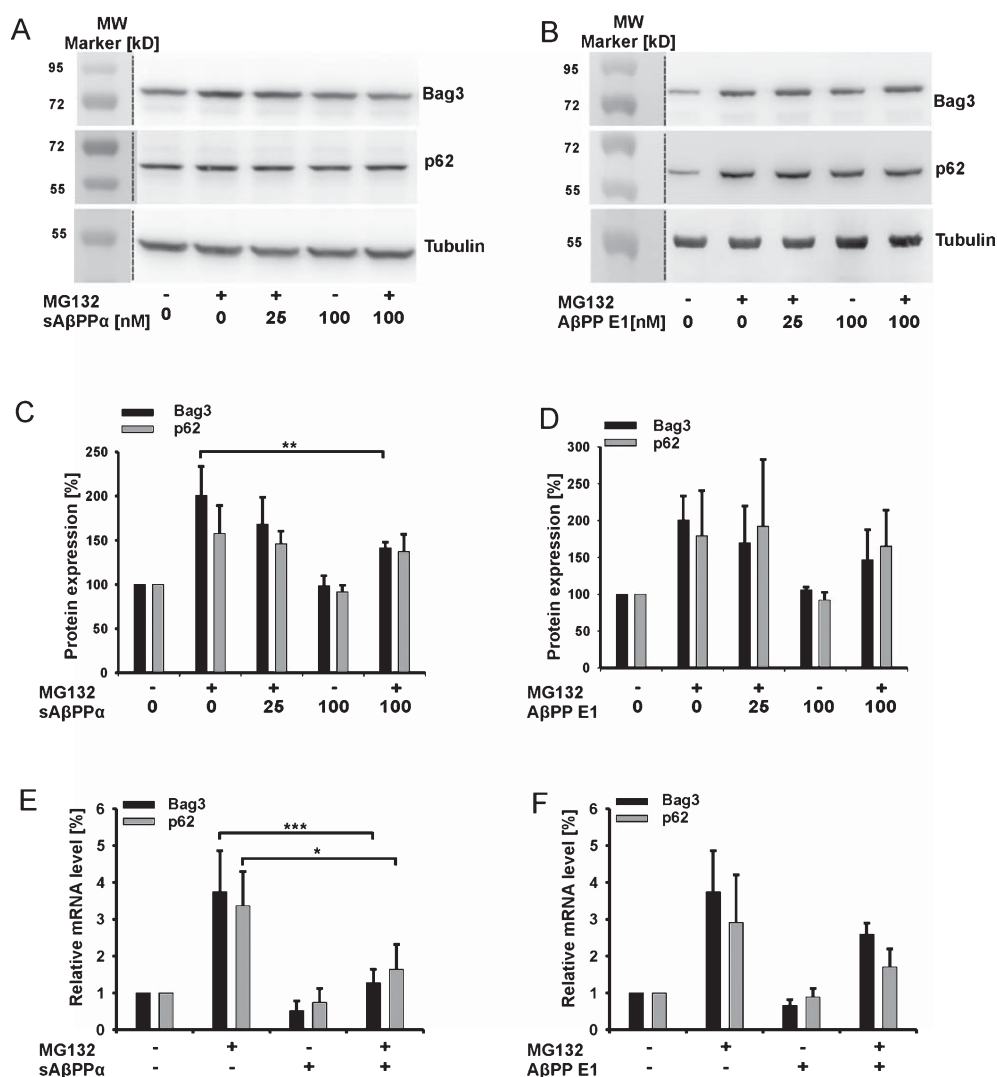
Fig. 4. sAβPPα significantly reduces Bag3 induction after proteasome inhibition in IMR90 cells, whereas a downstream member of autophagy p62 remained unaltered. Young IMR90 cells (PDL <30) were pre-incubated for 15 h with 100 nM concentration of (A, C) sAβPPα and (B, D) AβPP E1, prior to the addition of 0.5 μM MG-132. 24 h later, the cells were processed and analyzed by western blotting using anti-Bag3, anti-p62 and for control anti-tubulin antibodies as shown in (A, B). C, D) Densitometric quantification of the immunoreactive protein bands for Bag3 and p62, correspondingly. The absolute values measured were first normalized to tubulin and the resulting values were normalized to vehicle-treated control, which was set as 100%. E, F) Quantitative PCR analysis of the cells treated as in (A) and (B). All data represent mean ± SD from quadruplicate determinations. Asterisks indicate statistically significant differences versus MG-132-only treated cells: *$p \leq 0.05$; **$p \leq 0.01$; ***$p \leq 0.001$.

MG-132-induced increase in autophagic flux in young IMR90 cells treated with sAβPPα under proteasomal stress conditions (Fig. 5A, B). Nevertheless, this effect was not statistically significant.

sAβPPα prevents MG-132-induced perinuclear aggresome formation

Upon inhibition of the proteasomal degradation pathway, damaged or misfolded proteins accumulate and may form large perinuclear aggresomes and aggresome-targeted proteins are degraded by autophagy. Two proteins, Bag3 and vimentin, are well-described markers of aggresomes due to their direct localization to these perinuclear structures. We examined the effect of sAβPPα on aggresome formation in HEK 293 cells after proteasomal stress with MG-132. Immunocytochemistry for Bag3 demonstrated a significantly reduced protein level after treatment with sAβPPα (Fig. 6A, C). Moreover, aggre-
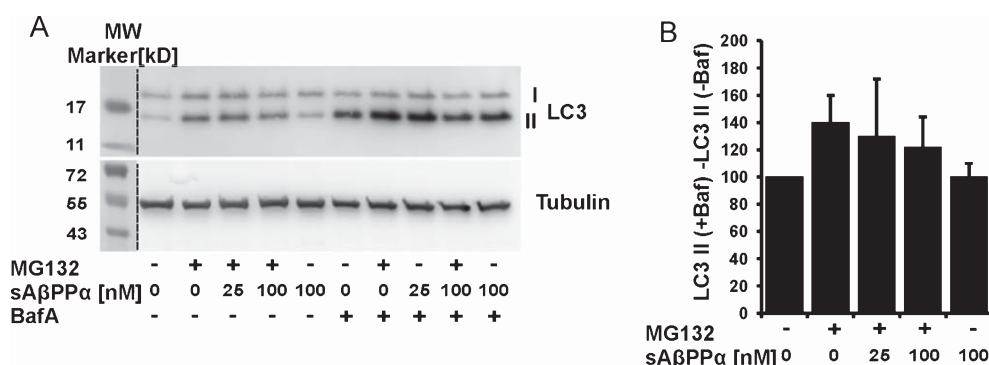
Fig. 5. Influence of sAβPPα on autophagic flux as measured by LC3-II. Young IMR90 cells (PDL <30) were pre-incubated for 15 h with 100 nM concentration of sAβPPα prior to the addition of 0.5 μM MG-132. 24 h later, the total cell lysates were processed and analyzed by western blotting using anti-LC3 antibody in the presence or absence of bafilomycin A. A) Representative blot from three independent experiments; (B) Quantification of LC3-II immunoreactive bands by subtracting LC3-II without bafilomycin treatment from LC3-II with bafilomycin treatment. The values were normalized to tubulin, which was used as a loading control. The data represent mean ± SD from triplicate determinations.

some formation was also analyzed by immunostaining of vimentin that is a well-established indicator of perinuclear aggresome formation. Under the conditions of increased autophagy, there was a strong aggregation and redistribution of the vimentin from cytosol to the perinuclear compartment detected indicating the formation of perinuclear aggresomes. Co-treatment with sAβPPα prevented MG-132-induced accumulation of vimentin-positive aggregates (Fig. 6B, D). In parallel, we quantified the protein levels of Bag3 and p62 under proteotoxic stress. Similar to IMR90 cells and primary neurons there was a significant reduction in Bag3 protein, whereas p62 remained mostly unchanged (Fig. 6E, F). The accumulation of LC3-II was likewise unchanged (Fig. 6G, H). Similar to IMR90 cells we could detect an increased cell survival in HEK 293 cells in the presence of sAβPPα under conditions of proteotoxic stress (Fig. 6I).

sAβPPα reduces mutant SOD1 protein aggregation

Our previous data revealed a significant reduction in aggresome formation in the presence of sAβPPα under conditions of proteotoxic stress. In order to further investigate the protective activity of sAβPPα in a disease-associated cell culture model, we employed cells expressing a mutant form of superoxide dismutase SOD1^{G85R} fused to GFP [25]. This mutation in SOD1 protein induces familial forms of amyotrophic lateral sclerosis (ALS), and mice overexpressing SOD1^{G85R} develop an ALS-like neuropathology that is associated with inclusion body formation in motor neurons of the spinal cord [26]. HEK 293 cells were transiently transfected with mutant SOD1-GFP

and subsequently immunostained with anti-vimentin. Mutant SOD1-GFP expressing cells showed cytoplasmic, pre-aggresomal, and aggresomal localization of SOD1^{G85R}-GFP. Inhibition of the proteasome with MG-132 increased the number of cells with pre-aggresomal and aggresomal mutant SOD1^{G85R}-GFP. Pre-treatment with sAβPPα significantly decreased the number of cells with aggresomal localization of mutant SOD1^{G85R}-GFP (Fig. 7A, B).

sAβPPα increases the activity of the proteasome

We have recently shown that in aged human cells the molecular switch from Bag1 to Bag3 goes along with an increase in macroautophagy and enhanced turnover of polyubiquitinated proteins [17]. So we examined the UPS activity by usage of HEK 293 cells stably expressing a GFP-based UPS reporter (d2-GFP). Degradation of d2-GFP was blocked by MG-132 and pre-treatment with sAβPPα induced an increase in degradation of d2-GFP (Fig. 8A, B). Employing a well-established substrate for the 20S proteasome, SUC-LLVY-AMC, we measured the activity of 20S by monitoring the consumption rate of this substrate. We found a higher activity of the 20S proteasome with sAβPPα under proteasomal stress conditions in young IMR90 cells and HEK 293 cells (Fig. 8C, E), whereas there was no change observed in aged IMR90 cells (Fig. 8D).

Based on our previously published finding on the reciprocal relationship of Bag3 and Bag1 expression [17], it was feasible to assume whether there was a change in the expression of Bag1 protein as a response to the observed Bag3 downregulation. But interestingly, analysis of all Bag1 variants, Bag1L, Bag1 M, Bag1, and Bag1S, revealed that there was no significant
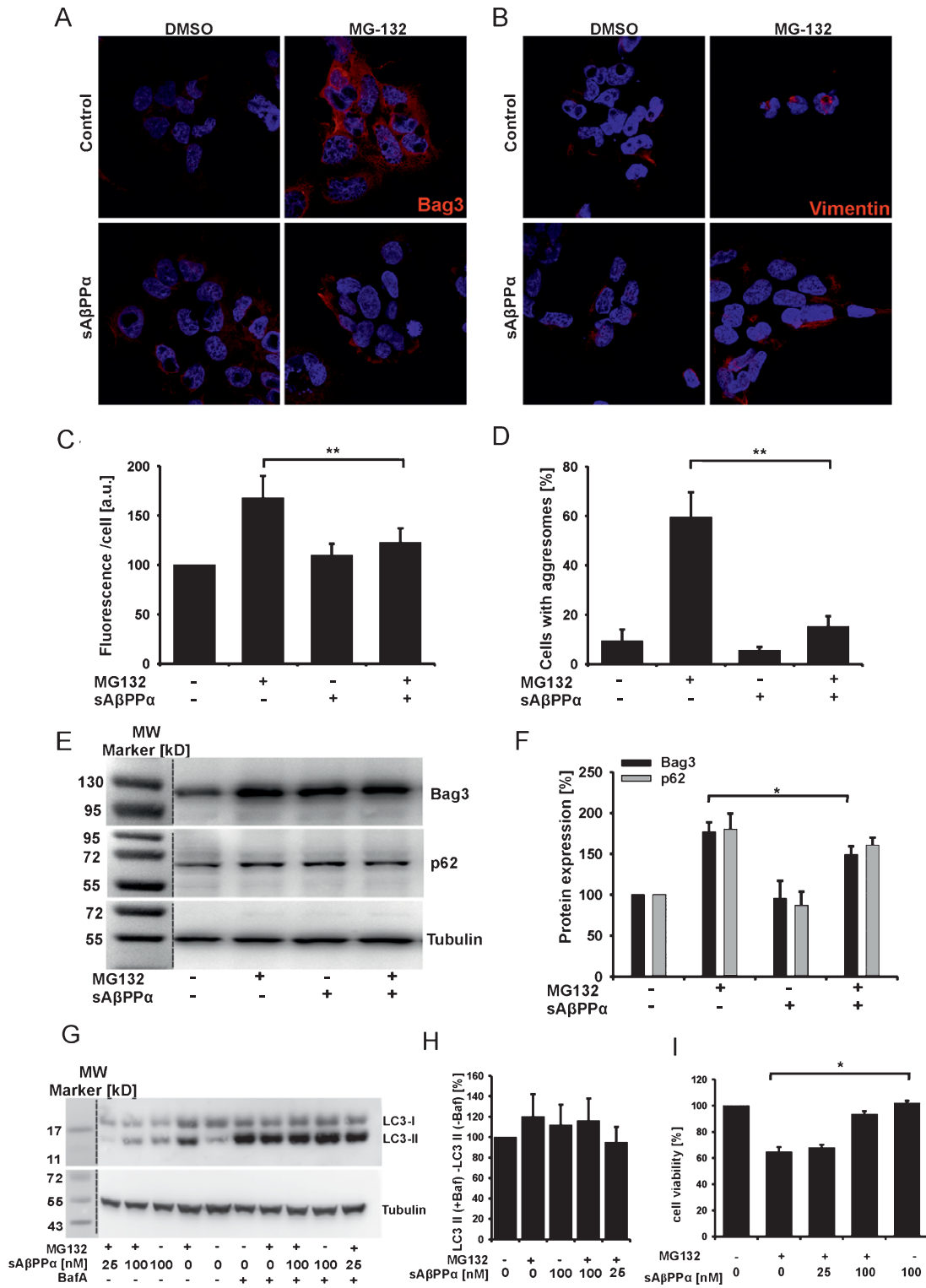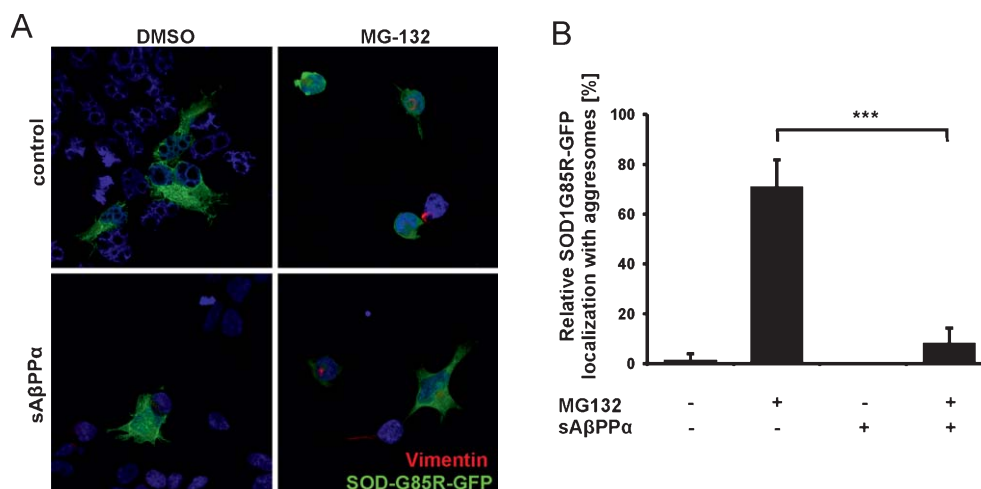
Fig. 7. sAβPPα decreases aggresome-targeting of substrates in HEK 293 cells. A) HEK 293 cells were transiently transfected with SOD^{G85R}-GFP. After 48 h cells were pre-treated with 100 nM sAβPPα 15 h prior to the administration of 0.5 μM MG-132 for 24 h. After that cells were fixed and immunostained with anti-vimentin and analyzed microscopically. Representative photographs of cells with cytoplasmic and SODG85R-GFP aggresome distribution are shown. Scale bar, 5 μm. B) Analysis and quantification of SOD^{G85R}-GFP (green) localization with aggresome marker vimentin by counting 5 random microscopic fields. Data represent mean ± SD from $n = 45$ cells. Statistically significant reduction of toxin-induced aggresome formation is indicated by asterisk: *** $p \leq 0.001$.

change in the expression of Bag1 proteins under these experimental conditions (Fig. 8F, G).

MG-132-induced protein ubiquitination is attenuated by sAβPPα

To understand whether the detected increase of proteasomal activity by sAβPPα is exerted by increased protein levels of the proteasome components, we ana-lyzed key players of the UPS: total ubiquitin, Nrf2, 19S proteasome, and 20S proteasome. Protein levels of these candidate proteins were investigated in young and aged IMR90 cells using western blot analysis. Our results demonstrate that in young IMR90 cells sAβPPα attenuate the MG-132-induced ubiquitin protein level (Fig. 9A, C) whereas in aged cells, sAβPPα had no impact on MG-132 induced protein ubiquiti-nation (Fig. 9B, D). Importantly, the protein levels of

Fig. 6. sAβPPα prevents MG-132-induced perinuclear aggresome formation in HEK 293 cells. HEK 293 cells were pre-treated with 100 nM sAβPPα and AβPP E1 or vehicle for 24 h before administration of 10 μM MG-132. After 8 h, the cells were fixed, immunostained with anti-Bag3 antibody and anti-vimentin antibody and subsequently analyzed microscopically. A, B) Representative pictures of the cells photographed at 200 x magnification. C) Quantification of fluorescence intensity of Bag3 immunofluorescence by automated image analysis of randomly taken photographs from each treatment, which was subsequently divided by the cell number using DAPI as a nuclear counterstain. The values were normalized to vehicle-treated control, which was set as 100%. Data represent mean ± SD. Statistically significant reduction of toxin-induced increase in Bag3 immunofluorescence is indicated by asterisk: ** $p \leq 0.01$. (a.u., arbitrary units). D) Quantification of randomly taken photographs from 10 μM MG-132-treated cells with or without sAβPPα by counting the cells with vimentin-positive aggresomes and subsequently normalizing the values to the number of cells, which was estimated by the number of nuclei (DAPI). Data represent mean ± SD from $n = 150$ cells. Statistically significant reduction of toxin-induced aggresome formation is indicated by asterisk: ** $p \leq 0.01$. E) HEK 293 cells were pre-treated with 100 nM sAβPPα 15 h prior to the administration of 0.5 μM MG-132 for 24 h. At this point, the cells were harvested and total cell lysates were analyzed by immunoblotting using antibodies against Bag3 and p62 as described in Materials and methods. Tubulin was used as a control for equal protein loading. F) Quantitative densitometric analysis of Bag3 and p62 signals in three independent experiments as presented in (E). The absolute values measured were first normalized to tubulin and the resulting values were normalized to vehicle-treated control, which was set as 100%. Significant differences versus toxin-only treated controls are marked by an asterisk; $p \leq 0.05$. G) HEK 293 cells were pre-treated with 100 nM sAβPPα prior to the administration of 0.5 μM MG-132 for 24 h with and without bafilomycin. After that cells were harvested and total cell lysates were analyzed using antibody against LC3. A representative LC3 and tubulin blots are shown where tubulin was used as a control for equal protein loading; (H) Densitometric analysis of LC3-II immunoreactive bands by normalizing the absolute values first to tubulin. Subsequently LC3-II signal without bafilomycin treatment was subtracted from LC3-II signal with bafilomycin treatment and the resulting values were normalized to vehicle-treated control, which was set as 100%. The data represent mean ± SD from triplicate determinations. I) HEK 293 cells were pre-treated with different concentrations of sAβPPα for 24 h. Afterwards cells were challenged with a proteasome inhibitor MG-132 for 48 h. Subsequently cells viability was determined using calorimetric MTT assay. The absolute values measured were normalized to untreated control, which was set as 100%. Significant differences versus toxin-only treated controls are marked by an asterisk; $p \leq 0.05$.
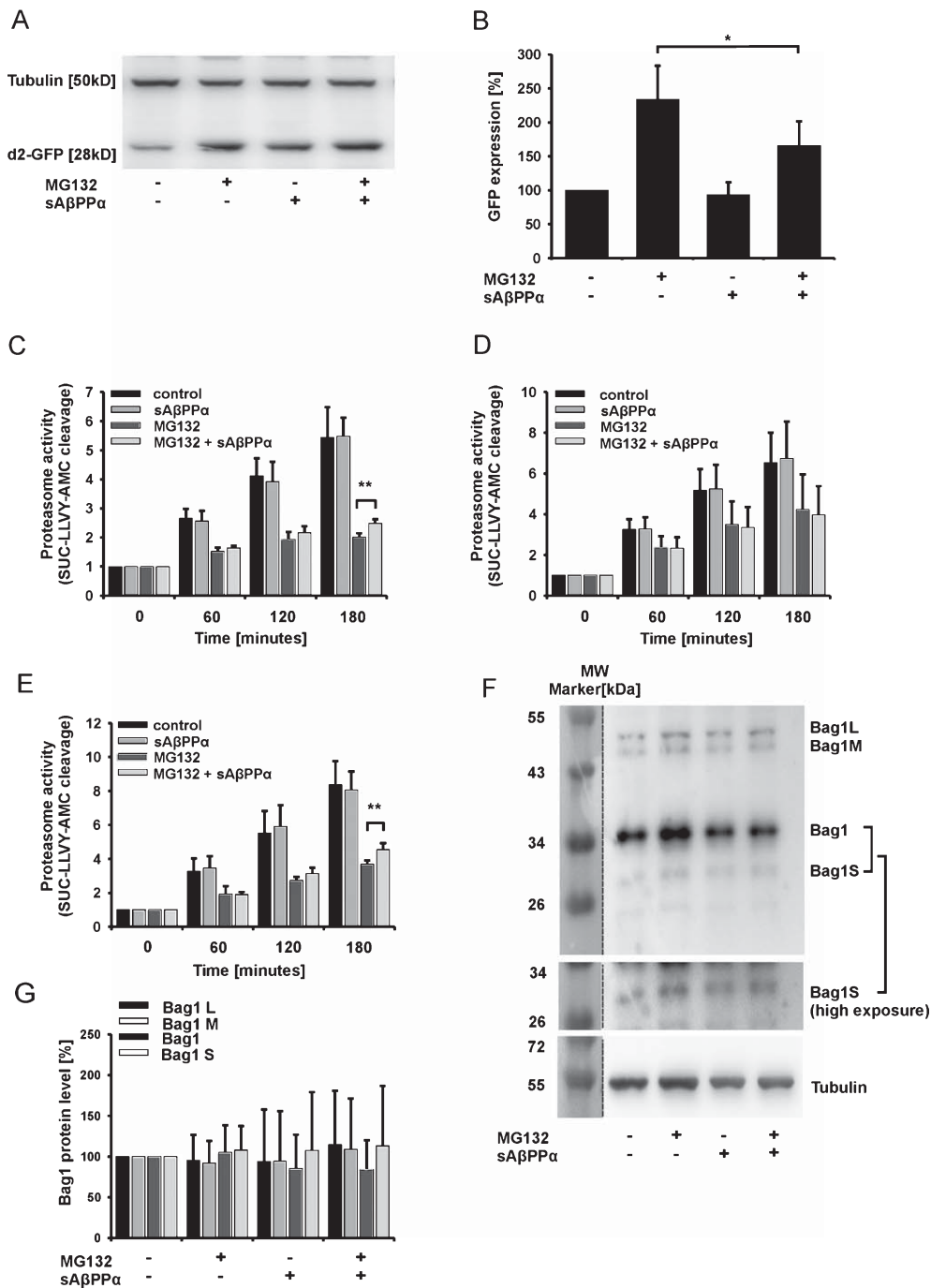
Fig. 8. sAβPPα increases proteasome activity under MG132 treatment. A) HEK 293 cells were transfected with d2-GFP reporter plasmid and pre-treated with 100 nM sAβPPα prior to addition of 0.5 μM MG-132. The cells were harvested and total lysates were analyzed by Western blotting using antibody against GFP. B) Quantification of the blot from (A) using densitometric analysis. C-E) Measurement of proteasome activity by means of SUC-assay, which represents the rate of SUC-LLVY-AMC cleavage as a proteasomal substrate in young IMR90 cells, aged IMR90 cells and HEK 293 cells, correspondingly. F) IMR90 cells were pre-treated with 100 nM sAβPPα and 15 h later were challenged with 0.5 μM MG-132. 24 h later, total protein lysates were analyzed by western blotting and detected using Bag1 antibody, which directed against the conserved BAG domain; Bag1S bands are shown separately in an immunoblot with a higher exposure. G) Densitometric analysis of Bag1L, Bag1 M, Bag1, and Bag1S immunoreactive bands. Data represent mean ± SD from quadruplicate determinations except (F) and (G), which represent mean ± SD from triplicate determinations. Statistically significant differences versus cells treated with MG-132 alone are indicated by asterisks:*$p \leq 0.05$ and **$p \leq 0.01$.
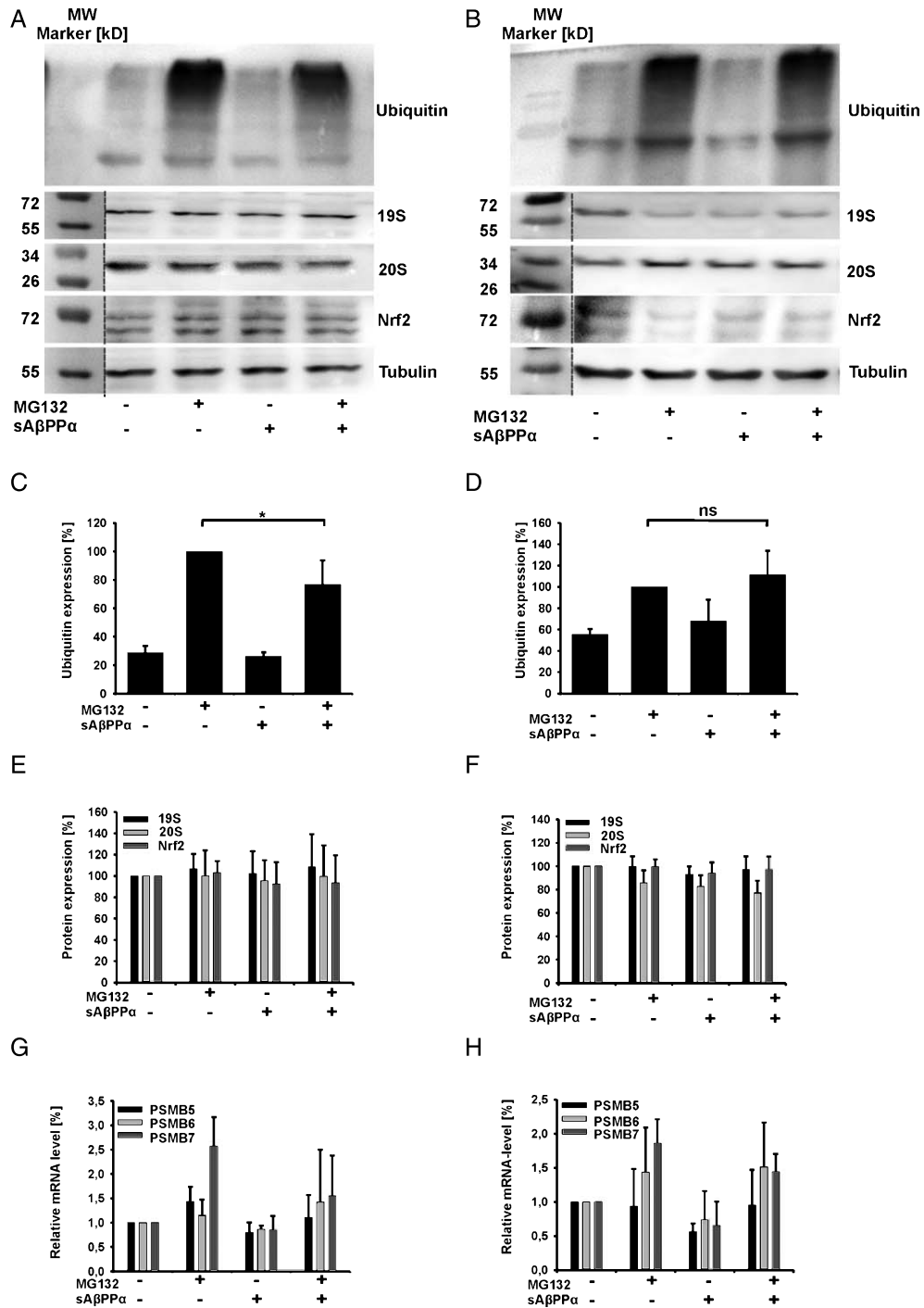
Fig. 9. sAβPPα decreases the levels of MG-132-induced protein ubiquitination. Young (A, C, E, G) and old IMR90 cells (B, D, F, H) were treated with 0.5 μM MG-132 for 24, with or without addition of 100 nM sAβPPα. After that total cell lysates were analyzed for total protein ubiquitin, 19S and 20S Proteasome and Nrf2 by western blotting. C, H) Densitometric quantification of the western blot analysis of (C, D) the ubiquitin levels, the (E, F) 19S, 20S and Nrf2 levels from young and old IMR90 cells, correspondingly. G, H) Quantitative PCR analysis of mRNA levels for components of proteasome PSMB5, PSMB6, and PSMB7. Data represent mean ± SD from triplicate determinations. Statistically significant differences versus MG-132 only-treated cells are indicated by asterisk: $^*p \leq 0.05$.

Nrf 2, 19S, and 20S proteasome remained unchanged in young and old IMR90 cells indicating a lack of regulation of these proteins by sAβPPα (Fig. 9A, B, E, F). Quantitative real-time PCR for PSMB5, PSMB6 and PSMB7, three subunits of the 20S proteasome also confirmed the lack of transcriptional regulation for sAβPPα in young and old IMR90 cells (Fig. 9G, H).

DISCUSSION

The non-amyloidogenic AβPP cleavage product sAβPPα is described to have neuroprotective and neurotrophic features [6, 7, 27–32]. Therefore, the decline of sAβPPα activity in AD patients might contribute to disease pathology. However, the knowledge about molecular pathways underlying these effects remains largely elusive.

Employing young and aged IMR90 cells, human HEK 293 cells, and primary mixed cortical and hippocampal neurons, we have demonstrated in this study that sAβPPα increases the proteasome activity under conditions of proteotoxic stress. Using a well-established proteasome inhibitor MG-132, we observed a significant transcriptional induction of Bag3 protein, which was suppressed by sAβPPα. Moreover, we observed a significant amelioration in cell survival under these conditions as it was determined by a metabolic MTT assay (Fig. 1C).

sAβPPα is an N-terminal fragment of the AβPP, which is processed by α-secretase ADAM10 via a so-called non-amyloidogenic pathway. Under physiological conditions, the majority of the predominant isoform of AβPP695 is processed by α-secretase. However, during aging and under certain pathological stress conditions, there is a molecular switch from non-amyloidogenic to amyloidogenic pathway leading to the accumulation of the toxic cleavage products of AβPP [7].

Despite the fact that sAβPPα is a preferential cleavage product of AβPP, the physiological function of this fragment is not yet fully understood. There are several studies reporting that sAβPPα can antagonize neuronal apoptosis [33]. Earlier works propose a role of sAβPPα in modulation of ion homeostasis by modulating ion channel function. sAβPPα was described to activate potassium channels and to suppress NMDA currents to limit Ca^{2+} overload and excitotoxic damage in neurons [34–36]. There are two regions in the sequence of sAβPPα that are proposed to be responsible for its neuroprotective and neurotrophic features: the N-terminal E1 domain and the E2 domain, both containing heparin binding activity, whereas the E2 domain is largely ineffective [12]. The neuroprotective ability of E1 domain is thought to be mediated by its heparin binding site [37]. The ability of this domain to bind heparin sulphate proteoglycans is thought to promote neurite outgrowth from central and peripheral neurons [38]. This could potentially induce physiologically important cell signaling events, which are not yet fully elucidated [39]. Furthermore, an antibody that binds to this region inhibited sAβPPα mediated synapse formation [40] and abolishes depolarization-induced neurite outgrowth [41].

In our present investigation, we employed the full length sAβPPα and its N-terminal E1 domain (AβPP E1). Given that AβPP E1 contains only one heparin-binding domain as compared to full length sAβPPα and assuming that the heparin-binding domain is involved in sAβPPα protective effects, we hypothesized that the effect of AβPP E1 might be weaker than that of sAβPPα. Therefore, we considered it as a suitable control to investigate the cellular effects of sAβPPα. As expected, the modulatory effects of AβPP E1 throughout all experiments in this study were basically similar to that of sAβPPα, but much weaker than the significant effects of sAβPPα.

Recent investigations on the role of autophagy in the pathogenesis of AD found a number of macroautophagic markers such as Atg5, Atg12, and LC3 to be associated with plaque and neurofibrillary tangles in AD [42–45]. Studies in an AβPP overexpressing cell line as well as mouse models reveal that AβPP and Aβ peptides localize with LC3 positive autophagosomes [46, 47]. Important members of the cross-talk between UPS and autophagy are thought to be the co-chaperone proteins Bag1 and Bag3 [48]. Our recent work demonstrates a prevalence of the autophagy pathway over UPS in naturally aged cells and brain tissue [17].

The maintenance of the intracellular protein homeostasis by degrading damaged and unfolded proteins is essential for cellular viability and function. There are two major protein degradation pathways in the cell responsible for stress-induced and constitutive protein turnover: the UPS and autophagy. Both systems provide a fine-tuned regulation of the cellular protein quality control. Impairment of interplay between these two pathways might lead to an accumulation of damaged and unfolded proteins. The impairment of protein quality control at different stages may lead to excessive accumulation of such proteins in the cell and is thought to be associated with neurodegeneration [45, 49].

We focused our study on the effect of sAβPPα on protein degradation machinery. Employing a

well-established model of replicative senescence IMR90 cells, we have demonstrated a modulatory function for sAβPPα on protein degradation machinery under conditions of proteotoxic stress. Interestingly, these positive influences of sAβPPα were observed in young, but not in aged cells. Although the induction of Bag3 with a proteasome inhibitor (MG-132) in aged cells was comparable with that in young cells, sAβPPα was unable to prevent this effect (Fig. 2). This finding suggests a differential role for sAβPPα in modulation of the transcription of Bag3 in young and aged cells. This could be due to the age-associated occurrence of irreversible changes to the proteasome complex. Moreover, numerous earlier studies demonstrate significant structural changes to proteasome complex either due to the oxidation of its single subunits or due to their disturbed assembly (for review, see [50]).

Interestingly, other components of the macroautophagy pathway such as p62 and LC3-II remain largely unaltered in these experiments (Figs. 4 and 5). In order to investigate the neuronal relevance of measured effects of sAβPPα on proteasome, we extended our investigations to neuronal cells. Employing primary hippocampal or cortical neurons, we indeed found effects of sAβPPα on the proteotoxic stress induced Bag3 expression fully comparable to those observed in IMR90 cells and HEK 293 cells (Fig. 3).

The involvement of Bag3 was further observed in perinuclear aggresomes induced by a proteasome inhibitor MG-132. Immunocytochemistry analysis revealed a strong accumulation of Bag3-positive aggresomes, which was significantly reduced by sAβPPα (Fig. 6A, C). Furthermore, there was a significant reduction of mutant SOD1 aggregation (Fig. 7). Incidentally, SOD1^{G85R} has been previously shown to be prone to aggregation [51, 52]. It is plausible to assume that a pharmacological inhibition of proteasome by MG-132 leads to induction of Bag-3 mediated macroautophagy. This is thought to be an adaptation strategy of the cells in order to control efficient protein turnover. Surprisingly, sAβPPα prevented this effect by downregulating the expression of Bag3.

In order to understand this finding that may occur counterintuitive to some extent, we had a closer look into the other component of protein degradation, the proteasome. Employing well-established substrates for a proteasome such as degradation of d2-GFP and SUC-LLVY-AMC, we observed a significant enhancement of the proteasomal activity in the presence of sAβPPα in two cell systems. The amount of the ubiquitinated proteins, which is a well-accepted marker for cellular

proteasome activity, was also significantly decreased (Fig. 8A-D). Interestingly, sAβPPα had no effect on the protein levels of the key components of the proteasome such as 19S and 20S as well as three important subunits of 20S proteasome, PSMB5, PSMB6, and PSMB7, indicating a direct modulation of the sAβPPα protective in post-translational fashion. Based on our previous findings demonstrating the presence of a reciprocal relationship between Bag3 and Bag1 proteins, it was plausible to assume that sAβPPα-induced decrease in Bag3 may partially lead to a compensatory increase in expression of Bag1. Interestingly, the analysis of total Bag1 protein family (Bag1L, Bag1 M, Bag1, and Bag1S) demonstrated that Bag1 was largely unaffected under these experimental conditions (Fig. 8F, G).

Since Bag3-mediated macroautophagy is one of the important adaptive responses of the cells under conditions of proteotoxic stress, an alternative interpretation of the observed effects of sAβPPα is that sAβPPα-induced increase in proteasome activity may prevent the induction of Bag3 protein. It is well accepted that constitutive autophagy plays a central role in the elimination of unfavorable proteins, independent of the proteasome system. However, it is not known so far whether autophagy and proteasome degradation target a similar set of normal and/or misfolded proteins. It is plausible that due to a high energy demand the autophagic pathway assists in degrading accumulated proteins when cellular levels of aberrant proteins overwhelm the disposal capacity of the proteasome. Therefore, we assume that the cells may descend the need to induce Bag3-mediated autophagy under the conditions of increased proteasome activity.

In conclusion, our study suggests that the effect of sAβPPα is exerted at least partly through the modulation of the proteasome activity. These data provide insights into the molecular pathways downstream of sAβPPα and suggests a novel function for this AβPP cleavage product. Moreover, we demonstrate that sAβPPα may have differential effects in young and aged cells.

An interesting question arising in this context is how sAβPPα being a soluble extracellular protein fragment of AβPP affects intracellular proteostasis. A previous elaborated publication demonstrated that sorting protein-related receptor containing LDLR class A repeats (SORLA or LR11) may act as sAβPPα receptors [53]. Others reported that sAβPPα might modulate membrane tethered AβPP dimerization, which might trigger the intracellular signaling [54]. However, future experiments will be required to decipher the

intracellular molecular mechanisms underlying the protective sAβPPα activity.

ACKNOWLEDGMENTS

REFERENCES

[1] Sperling RA, Aisen PS, Beckett LA, Bennett DA, Craft S, Fagan AM, Iwatsubo T, Jack CR Jr, Kaye J, Montine TJ, Park DC, Reiman EM, Rowe CC, Siemers E, Stern Y, Yaffe K, Carrillo MC, Thies B, Morrison-Bogorad M, Wagster MV, Phelps CH (2011) Toward defining the preclinical stages of Alzheimer's disease: Recommendations from the National Institute on Aging-Alzheimer's Association workgroups on diagnostic guidelines for Alzheimer's disease. *Alzheimers Dement* **7**, 280-292.

[2] Montine TJ, Phelps CH, Beach TG, Bigio EH, Cairns NJ, Dickson DW, Duyckaerts C, Frosch MP, Masliah E, Mirra SS, Nelson PT, Schneider JA, Thal DR, Trojanowski JQ, Vinters HV, Hyman BT; National Institute on Aging; Alzheimer's Association (2012) National Institute on Aging-Alzheimer's Association guidelines for the neuropathologic assessment of Alzheimer's disease: A practical approach. *Acta Neuropathol* **123**, 1-11.

[3] Haass C, Kaether C, Thinakaran G, Sisodia S (2012) Trafficking and proteolytic processing of APP. *Cold Spring Harb Perspect Med* **2**, a006270.

[4] Bredesen DE (2009) Neurodegeneration in Alzheimer's disease: Caspases and synaptic element interdependence. *Mol Neurodegener* **4**, 27.

[5] Tian Y, Crump CJ, Li YM (2010) Dual role of alpha-secretase cleavage in the regulation of gamma-secretase activity for amyloid production. *J Biol Chem* **285**, 32549-32556.

[6] Bell KF, Zheng L, Fahrenholz F, Cuello AC (2008) ADAM-10 over-expression increases cortical synaptogenesis. *Neurobiol Aging* **29**, 554-565.

[7] Kögel D, Deller T, Behl C (2012) Roles of amyloid precursor protein family members in neuroprotection, stress signaling and aging. *Exp Brain Res* **217**, 471-479.

[8] Palmert MR, Usiak M, Mayeux R, Raskind M, Tourtellotte WW, Younkin SG (1990) Soluble derivatives of the beta amyloid protein precursor in cerebrospinal fluid: Alterations in normal aging and in Alzheimer's disease. *Neurology* **40**, 1028-1034.

[9] Lannfelt L, Basun H, Wahlund LO, Rowe BA, Wagner SL (1995) Decreased alpha-secretase-cleaved amyloid precursor protein as a diagnostic marker for Alzheimer's disease. *Nat Med* **1**, 829-832.

[10] Sennvik K, Fastbom J, Blomberg M, Wahlund LO, Winblad B, Benedikz E (2000) Levels of alpha- and beta-secretase cleaved amyloid precursor protein in the cerebrospinal fluid of Alzheimer's disease patients. *Neurosci Lett* **278**, 169-172.

[11] Fahrenholz F, Postina R (2006) Alpha-secretase activation-an approach to Alzheimer's disease therapy. *Neurodegener Dis* **3**, 255-261.

[12] Corrigan F, Pham CL, Vink R, Blumbergs PC, Masters CL, van den Heuvel C, Cappai R (2011) The neuroprotective domains of the amyloid precursor protein in traumatic brain injury, are located in the two growth factor domains. *Brain Res* **1378**, 137-143.

[13] Schubert D, Behl C (1993) The expression of amyloid beta protein precursor protects nerve cells from beta-amyloid and glutamate toxicity and alters their interaction with the extracellular matrix. *Brain Res* **629**, 275-282.

[14] Sarker D, Reid AH, Yap TA, de Bono JS (2009) Targeting the PI3K/AKT pathway for the treatment of prostate cancer. *Clin Cancer Res* **15**, 4799-4805.

[15] Eckert GP, Chang S, Eckmann J, Copanaki E, Hagl S, Hener U, Müller WE, Kögel D (2011) Liposome-incorporated DHA increases neuronal survival by enhancing non-amyloidogenic APP processing. *Biochim Biophys Acta* **1808**, 236-243.

[16] Wang HQ, Liu BQ, Gao YY, Meng X, Guan Y, Zhang HY, Du ZX (2009) Inhibition of the JNK signalling pathway enhances proteasome inhibitor-induced apoptosis of kidney cancer cells by suppression of BAG3 expression. *Br J Pharmacol* **158**, 1405-1412.

[17] Gamerdinger M, Hajieva P, Kaya AM, Wolfrum U, Hartl FU, Behl C (2009) Protein quality control during aging involves recruitment of the macroautophagy pathway by BAG3. *EMBO J* **28**, 889-901.

[18] Pimplikar SW, Nixon RA, Robakis NK, Shen J, Tsai LH (2010) Amyloid-independent mechanisms in Alzheimer's disease pathogenesis. *J Neurosci* **30**, 14946-14954.

[19] Hajieva P, Mocko J, Moosmann B, Behl C (2009) Novel imine antioxidants at low nanomolar concentrations protect dopaminergic cells from oxidative neurotoxicity. *J Neurochem* **110**, 118-132.

[20] Brendel A, Renziehausen J, Behl C, Hajieva P (2014) Down-regulation of PMCA2 increases the vulnerability of midbrain neurons to mitochondrial complex I inhibition. *Neurotoxicology* **40**, 43-51.

[21] Nichols WW, Murphy DG, Cristofalo VJ, Toji LH, Greene AE, Dwight SA (1977) Characterization of a new human diploid cell strain, IMR-90. *Science* **196**, 60-63.

[22] Kern A, Roempp B, Prager K, Walter J, Behl C (2006) Down-regulation of endogenous amyloid precursor protein processing due to cellular aging. *J Biol Chem* **281**, 2405-2413.

[23] Pankiv S, Clausen TH, Lamark T, Brech A, Bruun JA, Outzen H, Øvervatn A, Bjørkøy G, Johansen T (2007) p62/SQSTM1 binds directly to Atg8/LC3 to facilitate degradation of ubiquitinated protein aggregates by autophagy. *J Biol Chem* **282**, 24131-24145.

[24] González-Polo RA, Boya P, Pauleau AL, Jalil A, Larochette N, Souquère S, Eskelinen EL, Pierron G, Saftig P, Kroemer G (2005) The apoptosis/autophagy paradox: Autophagic vacuolization before apoptotic death. *J Cell Sci* **118**(Pt 14), 3091-3102.

[25] Gamerdinger M, Kaya AM, Wolfrum U, Clement AM, Behl C (2011). BAG3 mediates chaperone-based aggresome-targeting and selective autophagy of misfolded proteins. *EMBO Rep* **12**, 149-156.

[26] Johnston JA, Dalton MJ, Gurney ME, Kopito RR (2000) Formation of high molecular weight complexes of mutant Cu, Zn-superoxide dismutase in a mouse model for familial amyotrophic lateral sclerosis. *Proc Natl Acad Sci U S A* **97**, 12571-12576.

[27] Meziane H, Dodart JC, Mathis C, Little S, Clemens J, Paul SM, Ungerer A (1998) Memory enhancing effects of secreted forms of the beta-amyloid precursor protein in normal and amnestic mice. *Proc Natl Acad Sci U S A* **95**, 12683-12688.

[28] Araki W, Kitaguchi N, Tokushima Y, Ishii K, Aratake H, Shimohama S, Nakamura S, Kimura J (1991) Trophic effect of beta-amyloid precursor protein on cerebral cortical neurons in culture. *Biochem Biophys Res Commun* **181**, 265-271.

[29] Qiu WQ, Ferreira A, Miller C, Koo EH, Selkoe DJ (1995) Cell-surface beta amyloid precursor protein stimulates neurite outgrowth of hippocampal neurons in an isoform-dependent manner. *J Neurosci* **15**, 2157-2167.

[30] Mattson MP, Cheng B, Culwell AR, Esch FS, Lieberburg I, Rydel RE (1993) Evidence for excitoprotective and intraneuronal calcium-regulating roles for secreted forms of the beta-amyloid precursor protein. *Neuron* **10**, 243-254.

[31] Postina R, Schroeder A, Dewachter I, Bohl J, Schmitt U, Kojro E, Prinzen C, Endres K, Hiemke C, Blessing M, Flamez P, Dequenne A, Godaux E, van Leuven F, Fahrenholz F (2004) A disintegrin-metalloproteinase prevents amyloid plaque formation and hippocampal defects in an Alzheimer disease mouse model. *J Clin Invest* **113**, 1456-1464.

[32] Stein TD, Anders NJ, DeCarli C, Chan SL, Mattson MP, Johnson JA (2004) Neutralization of transthyretin reverses the neuroprotective effects of secreted amyloid precursor protein (APP) in APPSW mice resulting in tau phosphorylation and loss of hippocampal neurons: Support for the amyloid hypothesis. *J Neurosci* **24**, 7707-7717.

[33] Kögel D, Concannon CG, Müller T, König H, Bonner C, Poeschel S, Chang S, Egensperger R, Prehn JH (2012b) The APP intracellular domain (AICD) potentiates ER stress-induced apoptosis. *Neurobiol Aging* **217**, 471-479.

[34] Furukawa K, Barger SW, Blalock EM, Mattson MP (1996) Activation of *K+* channels and suppression of neuronal activity by secreted beta-amyloid-precursor protein. *Nature* **379**, 74-78.

[35] Mattson MP (1997) Cellular actions of beta-amyloid precursor protein and its soluble and fibrillogenic derivatives. *Physiol Rev* **77**, 1081-1132.

[36] Furukawa K, Mattson MP (1998) Secreted amyloid precursor protein alpha selectively suppresses N-methyl-D-aspartate currents in hippocampal neurons: Involvement of cyclic GMP. *Neuroscience* **83**, 429-438.

[37] Rossjohn J, Cappai R, Feil SC, Henry A, McKinstry WJ, Galatis D, Hesse L, Multhaup G, Beyreuther K, Masters CL, Parker MW (1999) Crystal structure of the N-terminal, growth factor-like domain of Alzheimer amyloid precursor protein. *Nat Struct Biol* **6**, 327-331.

[38] Small DH, Nurcombe V, Reed G, Clarris H, Moir R, Beyreuther K, Masters CL (1994) A heparin-binding domain in the amyloid protein precursor of Alzheimer's disease is involved in the regulation of neurite outgrowth. *J Neurosci* **14**, 2117-2127.

[39] Reinhard C, Hebert SS, De Strooper B (2005) The amyloid-beta precursor protein: Integrating structure with biological function. *EMBO J* **24**, 3996-4006.

[40] Morimoto T, Ohsawa I, Takamura C, Ishiguro M, Nakamura Y, Kohsaka S (1998) Novel domain-specific actions of amyloid precursor protein on developing synapses. *J Neurosci* **18**, 9386-9393.

[41] Gakhar-Koppole N, Hundeshagen P, Mandl C, Weyer SW, Allinquant B, Muller U, Ciccolini F (2008) Activity requires soluble amyloid precursor protein alpha to promote neurite outgrowth in neural stem cell-derived neurons via activation of the MAPK pathway *Eur J Neurosci* **28**, 871-882.

[42] Pickford F, Masliah E, Britschgi M, Lucin K, Narasimhan R, Jaeger PA, Small S, Spencer B, Rockenstein E, Levine B, Wyss-Coray T (2008) The autophagy-related protein beclin 1 shows reduced expression in early Alzheimer disease and regulates amyloid beta accumulation in mice. *J Clin Invest* **118**, 2190-2199.

[43] Jaeger PA, Pickford F, Sun CH, Lucin KM, Masliah E, Wyss-Coray T (2010) Regulation of amyloid precursor protein processing by the Beclin 1 complex. *PLoS One* **5**, e11102.

[44] Ma JF, Huang Y, Chen SD, Halliday G (2010) Immunohistochemical evidence for macroautophagy in neurones and endothelial cells in Alzheimer's disease. *Neuropathol Appl Neurobiol* **36**, 312-319.

[45] Morawe T, Hiebel C, Kern A, Behl C (2012) Protein homeostasis, aging and Alzheimer's disease. *Mol Neurobiol* **46**, 41-54.

[46] Yu WH, Kumar A, Peterhoff C, Shapiro Kulnane L, Uchiyama Y, Lamb BT, Cuervo AM, Nixon RA (2004) Autophagic vacuoles are enriched in amyloid precursor protein-secretase activities: Implications for beta-amyloid peptide over-production and localization in Alzheimer's disease. *Int J Biochem Cell Biol* **36**, 2531-2540.

[47] Lunemann JD, Schmidt J, Schmid D, Barthel K, Wrede A, Dalakas MC, Munz C (2007) Beta-amyloid is a substrate of autophagy in sporadic inclusion body myositis. *Ann Neurol* **61**, 476-483.

[48] Gamerdinger M, Carra S, Behl C (2011) Emerging roles of molecular chaperones and co-chaperones in selective autophagy: Focus on BAG proteins. *J Mol Med (Berl)* **89**, 1175-1182.

[49] Nixon RA, Yang DS (2012) Autophagy failure in Alzheimer's disease–locating the primary defect. *Neurobiol Dis* **43**, 38-45.

[50] Höhn A, Grune T (2013) Lipofuscin: Formation, effects and role of macroautophagy. *Redox Biol* **1**, 140-144.

[51] Johnston JA, Dalton MJ, Gurney ME, Kopito RR (2000) Formation of high molecular weight complexes of mutant Cu, Zn-superoxide dismutase in a mouse model for familial amyotrophic lateral sclerosis. *Proc Natl Acad Sci U S A* **97**, 12571-12576.

[52] Witan H, Kern A, Koziollek-Drechsler I, Wade R, Behl C, Clement AM (2008) Heterodimer formation of wild-type and amyotrophic lateral sclerosis-causing mutant Cu/Zn-superoxide dismutase induces toxicity independent of protein aggregation. *Hum Mol Genet* **17**, 1373-1385.

[53] Hartl D, Klatt S, Roch M, Konthur Z, Klose J, Willnow TE, Rohe M (2013) Soluble alpha-APP (sAPPalpha) regulates CDK5 expression and activity in neurons. *PLoS One* **8**, e65920.

[54] Gralle M, Ferreira ST (2007) Structure and functions of the human amyloid precursor protein: The whole is more than the sum of its parts. *Prog Neurobiol* **82**, 11-32.